

[11] Real-Time Reporting of Circadian-Regulated Gene Expression by Luciferase Imaging in Plants and Mammalian Cells

By DAVID K. WELSH, TAKATO IMAIZUMI, and STEVE A. KAY

Abstract

Luciferase enzymes have been used as reporters of circadian rhythms in organisms as diverse as cyanobacteria, plants, fruit flies, and mice. This article details methodology for real-time reporting of circadian-regulated gene expression by imaging of luciferase bioluminescence in plants and mammalian cells.

Introduction

Luciferases are naturally occurring protein enzymes that catalyze emission of light from a substrate (luminescence). Many structurally heterogeneous forms of luciferase exist, in a wide range of species (Greer and Szalay, 2002). The best known is firefly luciferase, which catalyzes the emission of green (~560 nm) photons from its natural substrate, firefly luciferin, in the presence of oxygen and ATP. Many luciferases have relatively short half-lives of just a few hours, or even ~1 h in some cases (Leclerc *et al.*, 2000; Yamaguchi *et al.*, 2003), making them good reporters of changes in transcriptional rate on a circadian timescale. Genes for firefly luciferase and a few others have been cloned and are available commercially.

Luciferase luminescence is extremely dim, often too dim to be seen by the unaided eye in experimental applications. Various much brighter fluorescent reporters are available (Zhang *et al.*, 2002), and two of these have been used successfully to monitor circadian rhythms: green fluorescent protein (GFP) (Kuhlman *et al.*, 2000) and “Cameleon,” a sensor of cytoplasmic $[Ca^{2+}]$ (Ikeda *et al.*, 2003). Luciferase, however, enjoys two principal advantages over the fluorescent reporters. First, luciferase does not require exogenous illumination: the light detected is emitted from the biological sample itself. Fluorescent reporters, on the other hand, require bombardment with toxic, relatively high-energy photons, so that the reporter can be excited and then re-emit lower-energy photons. Over long-term circadian experiments, phototoxicity is a serious concern with fluorescent reporters but a nonissue with luciferase. Second, background emission of light by biological samples (or by luciferase substrate alone) is generally

extremely low, whereas autofluorescence background levels can be as high as the fluorescence signal of the reporter itself (Billinton and Knight, 2001). GFP fluorescence, for example, spectrally overlaps that of riboflavin (vitamin B₂), an essential enzyme cofactor found in biological tissues and culture media (Zylka and Schnapp, 1996). Thus, despite its modest photic output, luciferase is well suited as an optical reporter of circadian function.

The first use of a luciferase to monitor circadian function was in *Gonyaulax*, a marine dinoflagellate exhibiting a natural circadian rhythm of bioluminescence (Hastings, 1989). Subsequently, exogenous luciferase genes, under control of promoters conferring circadian regulation, have been introduced into a wide variety of organisms, including cyanobacteria (*Synechococcus*) (Kondo *et al.*, 1993), plants (*Arabidopsis*) (Millar *et al.*, 1992), insects (*Drosophila*) (Brandes *et al.*, 1996; Plautz *et al.*, 1997), and rodents (Asai *et al.*, 2001; Wilsbacher *et al.*, 2002; Yamaguchi *et al.*, 2003; Yamazaki *et al.*, 2000; Yoo *et al.*, 2004). These transgenic organisms exhibit robust (although quite dim) circadian rhythms of bioluminescence, useful for a wide range of genetic and biochemical studies of circadian clock mechanisms. In mammals, luciferase has been used to report circadian rhythms of gene expression in peripheral tissue explants (Yamazaki *et al.*, 2000), cultured suprachiasmatic nucleus (SCN) slices (Yamaguchi *et al.*, 2003), and even *in vivo* (Yamaguchi *et al.*, 2001). This article focuses on methodologies used in our laboratory for monitoring circadian output from plant seedlings and mammalian cells.

Plants

Vectors

For real-time monitoring of circadian rhythms in plants, we use *Arabidopsis thaliana* seedlings transgenic for the firefly luciferase gene, under control of a promoter conferring circadian transcription. The circadian promoter elements we use routinely are derived from the “*chlorophyll a/b* binding protein 2” (*cab2*) gene (Millar *et al.*, 1992) or the “*cold circadian rhythm RNA-binding 2*” (*ccr2*) gene (Strayer *et al.*, 2000). We use a modified luciferase sequence (*luc+*), available from Promega, which is 10–100× brighter than the native luciferase when expressed in plants. Binary vectors developed in our laboratory incorporate *luc+* as well as sequences necessary for delivery and expression of the gene in plants. Our standard *cab2* and *ccr2* reporter lines were created using the respective promoter elements, inserted into a promoterless vector (pATM-DOMega). For analysis of *cis* elements in promoters, we use a vector containing a minimal nopaline synthase (*nos*)

promoter (pATM-nos). The vectors, their sequences, and the transgenic plants are available upon request.

Plant Culture and Transformation

Seeds are surface sterilized with bleach and embedded into agar plates made with Murashige-Skoog (MS) salts (Caisson Labs MSP001), 3% sucrose, pH 5.8, in 8 g/L agar. Plants are grown under sterile conditions in an incubator set at 23° and entrained for 5–10 days to an LD 12:12 lighting cycle (12 h light, 12 h dark, light is 50–60 $\mu\text{mol}/\text{m}^2/\text{s}$ cool white fluorescent light). Plants are transformed using conventional agrobacterium-mediated methods (Clough and Bent, 1998), and transformants are selected by gentamycin or kanamycin drug resistance in MS agar plates with 75 mg/L gentamycin or 50 mg/L kanamycin.

Equipment and Reagents

To monitor luciferase activity, we use a “VIM” intensified charge-coupled device (CCD) camera equipped with an ARGUS-50 photon-counting imaging system (Hamamatsu). For some experiments, we have also used a “Night Owl” cooled CCD camera (EG&G Berthold). (See later for a discussion of state-of-the-art CCD cameras.) Depending on the desired field of view, we use wide-angle (17- or 35-mm) or standard (50-mm) photographic lenses mounted on the camera. The light-collecting ability of a photographic lens depends on its maximal aperture and is inversely proportional to the square of its *f* number (*f*), so lenses with low *f* are recommended [e.g., Schneider Kreuznach 17 mm (*f*/0.95), Nikon Nikkor 35 mm (*f*/1.4) or 50 mm (*f*/1.2)]. A light-tight black box is used for imaging, and the camera mount should have a light-tight single or double O-ring seal. Light leaks can be fixed with black RTV silicone rubber cement (Dow Corning) or black electrical tape.

As a substrate of luciferase, we use firefly D-luciferin (potassium salt, Biosynth L-8820). Luciferin is dissolved in dH₂O at 100 mM and stored in aliquots at –20° in the dark. A working solution (1–5 mM luciferin in 0.01% Triton X-100) is prepared and filter sterilized prior to the experiment. We use a small spray bottle to apply the working solution to plants.

Imaging

One day before starting the experiment, plants are pre-sprayed with 5 mM luciferin to reduce the background activity of accumulated luciferase (which is more stable in the absence of substrate). When imaging begins,

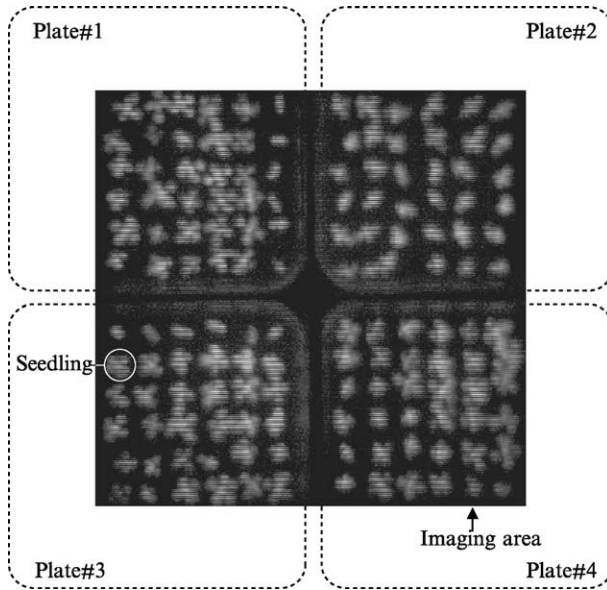


FIG. 1. Bioluminescent *Arabidopsis* seedlings. *Arabidopsis* seedlings transgenic for the bioluminescent reporter gene *cab2::luc* were grown for 2 weeks in square MS-agar plates (9.5×9.5 cm) and imaged using a VIM intensified CCD camera with an ARGUS-50 photon-counting imaging system (Hamamatsu). The imaging area (6×6 cm) includes portions of four plates and a total of 144 seedlings. This image was produced by accumulating photon counts over a 25-min exposure and then adding together 41 such exposures taken at 2.5-h intervals over a 4-day experiment.

plants are transferred to constant lighting conditions (constant white light, red light, blue light, or dark). At intervals of 2.5 h for 5 days, plants are temporarily moved to the light-tight black box for 25-min imaging sessions. Bioluminescence from up to 144 individual seedlings is captured by the camera in each 25-min exposure (Figs. 1 and 2). To ensure that luciferin substrate is not limiting, the plants are sprayed again before each time point with luciferin (5 mM on the first day and 1 mM thereafter).

Mammalian Cells

Methods for monitoring circadian rhythms of bioluminescence in mammalian cultures were pioneered by Shin Yamazaki in Michael Menaker's laboratory (Yamazaki *et al.*, 2000), and we follow the methodology he describes in the next article of this volume. Shun Yamaguchi, in Hitoshi Okamura's laboratory, extended these methods to allow imaging of single

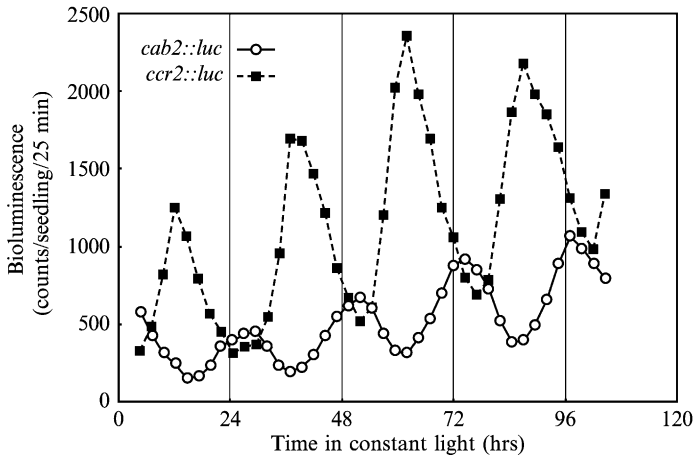


FIG. 2. Circadian rhythms of bioluminescence in *Arabidopsis* seedlings. Bioluminescence from individual *Arabidopsis* seedlings transgenic for either the *cab2::luc* or the *ccr2::luc* transgene was recorded over a 4-day experiment. Each data point represents photon counts from one seedling over a 25-min exposure. Note the higher amplitude and oppositely phased circadian rhythm in the *ccr2::luc* seedling compared with the *cab2::luc* seedling.

cells in SCN slices (Yamaguchi *et al.*, 2003) (see also Figs. 3 and 4). This section focuses on our optimization of these methods for studying dissociated cells (Welsh *et al.*, 2004; see also Figs. 5 and 6).

Reporter Design

Particularly for single cell studies, it is important to optimize circadian regulation of the luciferase reporter to ensure highly rhythmic expression in cells of interest. Several groups have used promoter sequences from the clock gene *mPer1* to drive expression of luciferase (Asai *et al.*, 2001; Wilsbacher *et al.*, 2002; Yamazaki *et al.*, 2000) or GFP (Kuhlman *et al.*, 2000) in transgenic rats or mice. However, *mPer1* may not be the best choice of promoter, as it appears dispensable for the expression of circadian rhythms at the molecular level (Bae *et al.*, 2001; Zheng *et al.*, 2001), and its expression may be less robust than *mPer2* in some SCN cells (Hamada *et al.*, 2001). Also, while random insertion may produce transgenic animals with multiple copies of the reporter and correspondingly higher levels of expression, there is always the worry that crucial but distant enhancer elements could be omitted or that sequences adjacent to the insertion site may interfere with expression. Indeed, constructs using longer *mPer1* promoter sequences appear to have produced more robust rhythmic expression. An *mPer2* knockin strategy, in which the endogenous rhythmic

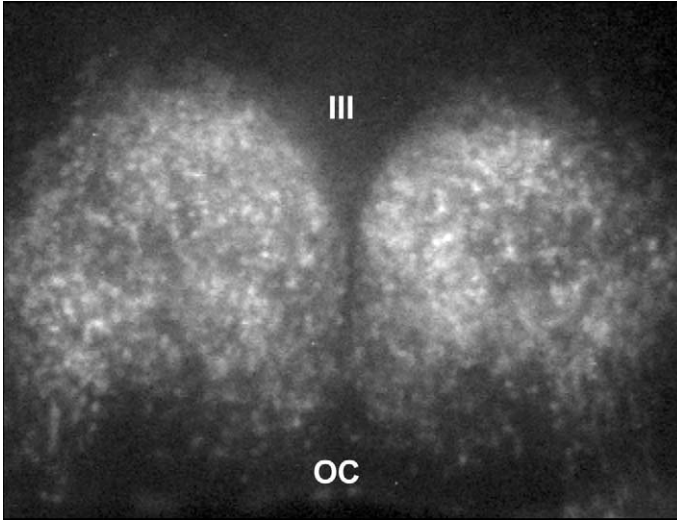


FIG. 3. Bioluminescent SCN slice from *mPer2::luc* knockin mouse. An SCN slice from a newborn *mPer2::luc* knockin mouse was cultured for 6 weeks in medium containing 1 mM luciferin. The slice was then imaged on an inverted Olympus IX70 microscope using a UPlanApo 10 \times objective and the Orca II ER cooled CCD camera (Hamamatsu), with 2 \times 2 binning. To eliminate spurious events, this image was constructed by pixel-by-pixel minimization of two consecutive 55-min exposures. Note the clear demarcation of luminescence from individual cells. III, 3rd ventricle. OC, optic chiasm.

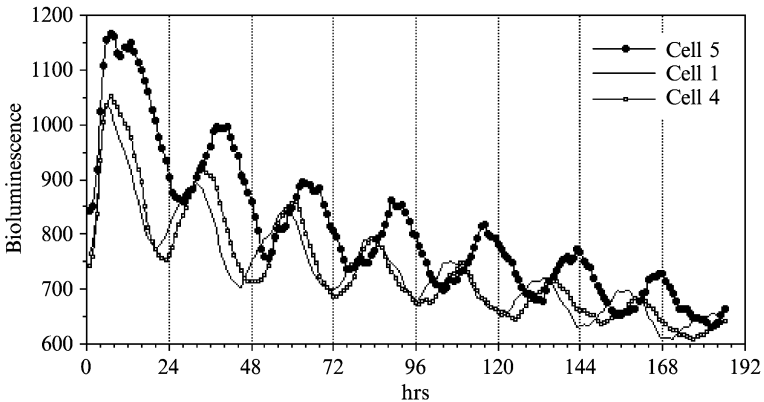


FIG. 4. Circadian rhythms of individual neurons in an SCN slice. Bioluminescence was recorded from individual neurons in an *mPer2::luc* SCN slice over an 8-day experiment. Each data point represents average luminescence intensity (in A/D units) within a single cell region of an image like that in Fig. 3. Note the clear circadian phase differences among cells.

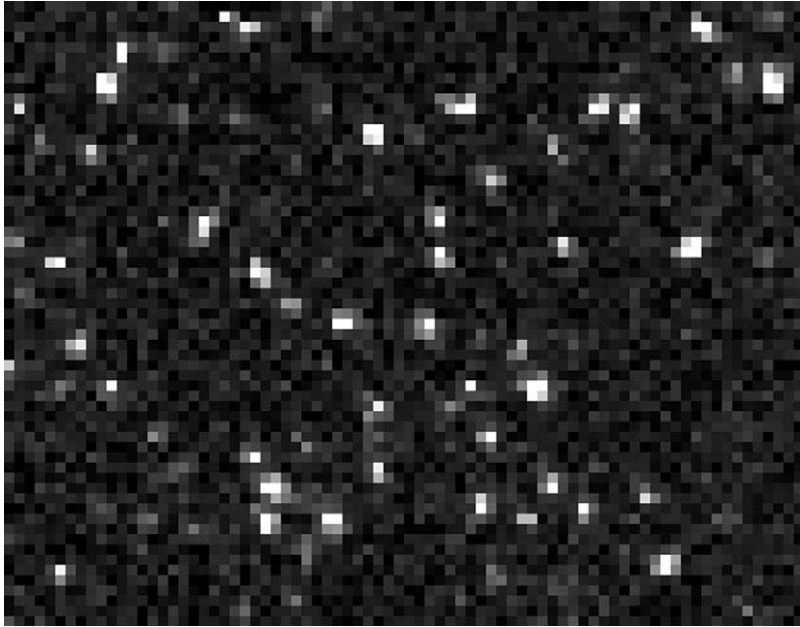


FIG. 5. Bioluminescent fibroblasts from an *mPer2::luc* knockin mouse. Primary fibroblasts were dissociated from the tail of a newborn *mPer2::luc* knockin mouse and cultured for 3 months in medium containing 1 mM luciferin. Cells were then imaged using a UPlanApo 4 \times objective and a Series 800 cooled CCD camera (Spectral Instruments), with 8 \times 8 binning. To eliminate spurious events, this image was constructed by pixel-by-pixel minimization of two consecutive 29.9-min exposures. The bright spots are individual cells. One pixel = 26 μ m.

mPer2 gene is replaced by a fusion of *mPer2* and *luc+*, obviates these concerns by coopting as much as possible of the endogenous, evolutionarily optimized transcriptional and translational regulation of mPER2. We therefore use the *mPer2::luc* knockin mice developed by Yoo *et al.* (2004).

Further improvements of reporter design will no doubt be made in the future. For instance, it might be possible to boost expression by the addition of exogenous enhancer elements (e.g., SV40). Brighter luciferases from other species (e.g., *Renilla*) or further enhancements of firefly luciferase (beyond *luc+*) may also prove useful. Most circadian reporter studies so far have introduced the reporter gene by germline transformation to create transgenic organisms with stable, uniform expression of the transgene. However, circadian reporters can be introduced into particular tissues or cells directly using adenovirus vectors (Lai *et al.*, 2002; Le Gal La Salle *et al.*, 1993) or other methods (Ikeda *et al.*, 2003), which may be more efficient in some cases.

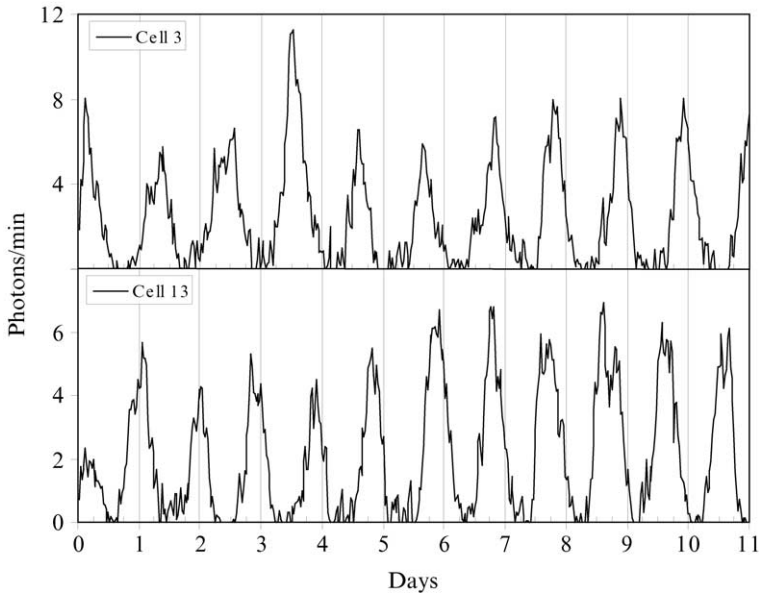


FIG. 6. Circadian rhythms of two individual fibroblasts. Bioluminescence was recorded from individual *mPer2::luc* fibroblasts over an 11-day experiment. Each data point represents total luminescence (in photons/min) within a single cell region of an image like that in Fig. 5. Values were converted from A/D units using the camera's specified gain and QE.

Tissue Culture

We culture tissue explants or dissociated cells in HEPES-buffered, air-equilibrated Dulbecco's Modified Eagle's Medium (DMEM) (GIBCO 12100-046) supplemented with 1.2 g/L NaHCO_3 , 10 mM HEPES, 4 mM gln, 25 U/ml penicillin, 25 $\mu\text{g/ml}$ streptomycin, and 2% B-27 (GIBCO 17504-044). Cells are placed in a 35-mm culture dish covered by a 40-mm circular coverslip (Erie Scientific 40CIR1), which is sealed in place with vacuum grease to prevent evaporation. Brain slices are cultured on Millicell-CM membrane inserts (Fisher PICMORG50). We add 1 mM luciferin (BioSynth L-8220) to the culture medium at the start of the experiment.

Luminometry

To monitor circadian rhythms of bioluminescence from cultures, we place the 35-mm dishes in a luminometer device constructed for this purpose (LumiCycle, Actimetrics, Inc.), which fits inside a standard tissue

culture incubator kept at 36°, 0% CO₂. The LumiCycle device is a light-tight box containing four photomultiplier tubes (PMTs; see [Table II](#)), hand-selected for low dark counts (10–40 Hz at 36°). Under the downward-gazing PMTs is a turntable with 32 slots for the 35-mm culture dishes. The turntable rotates four dishes at a time into position under the PMTs, and luminescence from each dish is measured for ~70 s at intervals of 10 min. The LumiCycle comes with analysis software that allows convenient plotting of luminescence rhythms, as well as computations of circadian period, phase, amplitude, damping rate, and magnitude of phase shifts (see later).

Microscopy

Single PMTs are highly sensitive detectors of photons, but of course they do not provide any spatial information; luminescence is measured from an entire dish at once. Many important questions about cellular organization of circadian clocks require longitudinal monitoring of circadian rhythms from single cells, which requires microscopic imaging.

Long-term luciferase imaging of single cells has been elusive until recently. One reason for this is the difficulty of maintaining fragile cell cultures on the microscope stage for long periods of time. We have solved this problem by use of a lucite chamber (Solent Scientific, UK) custom engineered to fit around the stage of our inverted microscope (Olympus IX70), which rests on an antivibration table (TMC). The environmental chamber keeps the stage at a constant 36°, with no focus drift. The chamber also accommodates gassing with 5% CO₂ for pH control of bicarbonate-buffered media, and the gas is thoroughly humidified to minimize evaporative loss. However, many cells do well in the simple configuration used for our luminometer experiments (HEPES-buffered, air-equilibrated DMEM medium, in a 35-mm culture dish sealed to prevent evaporation; see earlier discussion).

Maximizing the Signal

With healthy, luminescent cells on the microscope stage, the remaining challenge is to maximize the signal-to-noise ratio (S/N) so that the very dim luminescence of single cells can be detected ([Christenson, 2002](#)). This requires optimizing the chemistry of the luciferase reaction, the transmission of bioluminescence from sample to detector, and the sensitivity of the detector itself.

The bioluminescence signal should be maximized by optimizing conditions for the luciferase reaction. In the case of firefly luciferase, the substrate (luciferin) is quite hydrophilic and can be supplied in the culture

medium at saturating concentrations (1–5 mM). The brand of luciferin may be important, as some brands reportedly contain inhibitory by-products. We use 1 mM luciferin from BioSynth with good results. Temperature, [ATP], and [O₂] affect bioluminescence, but these are usually nearly optimal under standard tissue culture conditions.

Transmission of bioluminescence out of the culture dish should be maximized as well. Attenuation of the signal by phenol red in the culture medium may be up to 50% in a luminometer or upright microscope, where the detector is mounted above the culture dish (Erika Hawkins, Promega, personal communication) but is less significant in inverted microscopy, where the detector looks through only a thin film of medium. We use DMEM with phenol red (GIBCO 12100-046). For inverted microscopy, the underlying culture substrate is more of a concern. Millicell membranes are surprisingly transparent when wet, however. Glass or polystyrene culture vessels are also typically quite transparent, if they are clean.

Collection of photons by the objective lens must also be maximized. It is critical to use a lens with high light gathering power (LGP), which depends on numerical aperture (NA), magnification (Mag), and the mode of illumination:

$$\text{LGP for epifluorescence} = (\text{NA}^2/\text{Mag})^2 \times 10^4 \quad (1)$$

$$\text{LGP for luminescence} = (\text{NA}/\text{Mag})^2 \times 10^4 \quad (2)$$

Numerical aperture of a lens is defined as

$$\text{NA} = n \cdot \sin\theta, \quad (3)$$

where n is the refractive index of the medium between the lens and the sample and θ is the half-angle of the light cone collected by the lens. Note that LGP depends less on NA for luminescence (and for transmitted light) than it does for epifluorescence. This is because light passes through the lens twice for epifluorescence but only once for luminescence or transmitted light. Lower-magnification lenses have higher LGP because light is spread over fewer pixels at the detector; they also provide a greater field of view. Thus, a high-Mag lens with the highest available NA may be best for epifluorescence, but still not as good for luminescence as a lower Mag lens with more modest NA. See [Table I](#) for a list of suggested lenses.

The light gathered by an objective lens is still subject to reflective losses at all glass interfaces, both in the lens itself and beyond. The transmission of the lens is defined as the percentage of light gathered by the objective that is actually transmitted through it at a particular wavelength. In the past, reflective losses could be as great as 5% at each interface, and in high-quality

TABLE I
LIGHT-GATHERING POWER (LGP) OF LENSES SUGGESTED FOR LUCIFERASE IMAGING

Manufacturer	Name	Magnification	NA	NA/magnification	LGP
Nikon	Plan Apo	10×	0.45	0.045	20
Nikon	Plan Apo	4×	0.20	0.050	25
Olympus	UPlanApo	10×	0.40	0.040	16
Olympus	UPlanApo	4×	0.16	0.040	16
Olympus	XLFLUOR ^a	4×	0.28	0.070	49
Zeiss	FLUAR	10×	0.50	0.050	25
Zeiss	FLUAR	5×	0.25	0.050	25

^a Macro lens requires nonstandard mounting.

objective lenses with many elements for correction of spherical and chromatic aberration, the reflective losses could be as high as 50% overall. Thus, there was some advantage to using inexpensive lenses for luminescence applications because they had fewer lens elements and higher transmission. With recent advances in multilayer antireflection coating technology, however, this is no longer true: modern, high-quality lenses transmit more than 99.9% of the normal incidence light at visible wavelengths (see <http://www.microscopyu.com/articles/optics/objectiveproperties.html>). Furthermore, more expensive, highly corrected lenses tend to have higher NA (and thus higher LGP) for a given Mag.

Reflective losses beyond the objective should also be minimized. If the detector can be mounted on an inverted microscope with a bottom port (an unusual configuration), light can pass directly from the objective lens in a straight shot to the detector with no intervening mirror or other glass, which otherwise may attenuate the signal by 2–3% (R. Nazar, Olympus, personal communication). Of course, any glass surfaces that must remain in the optical path should be cleaned carefully, as dust specks or fingerprints can scatter considerable light.

Stray Light

It is also important to prevent extraneous light from reaching the detector. Even if stray light were reproducible in pattern and intensity so that it could be subtracted out from data images, it would still add greatly to the noise. The microscope should be located in a dark, windowless room, isolated by black curtains or a revolving light-tight door, with black walls and no phosphorescent paint or other materials. Equipment pilot lamps and LEDs should be covered by black electrical tape. Light leaks should be checked by eye after a 20-min dark adaptation. After positioning and

focusing the sample using bright-field illumination, the microscope can be turned off. For our inverted microscope (Olympus IX70), we also place a small (bottomless) black lucite box over the sample so that no light enters the lens from above the stage. As it is very difficult to completely eliminate extraneous light (e.g., LEDs inside computers), the microscope itself should be draped with blackout cloth (Thorlabs BK5). Computer monitors should be turned off during data acquisition. As a routine test, one can measure the noise (SD) of an image in the absence of a sample; this will increase if there are new light leaks.

Cameras

Perhaps the most critical decision for low-light luminescence microscopy is the choice of a highly sensitive, low-noise detector (Christenson, 2002). The best such devices are digital cameras, known as CCD cameras (see Web sites in Table II). These cameras rely on the photoelectric effect to detect light: incident photons liberate electrons from individual spots on a silicon chip, and the electrons are channeled in a controlled fashion so as to read out the number of electrons in each of these picture elements (pixels). The proportion of incident photons actually detected is known as the quantum efficiency (QE), which depends on wavelength (~560 nm for firefly luciferase). Due to thermal energy, some electrons are generated in the absence of incident photons, which is known as dark current, the fluctuation of which is dark noise. Dark current is proportional to exposure time, and therefore dark noise tends to predominate at the long exposure times required for very dim samples. There is also some uncertainty in the readout process itself, which is known as read noise. Thus, it is crucial to choose a CCD camera with high QE at 560 nm, low dark current, and low read noise.

Noise of a CCD camera can be measured as follows. First, to estimate total camera noise (N_{camera}), take a long exposure with the camera shuttered and calculate the standard deviation (SD) of pixel intensity values across the image. This is the “root-mean-squared” (rms) noise. Then, to

TABLE II
WEB SITES PROVIDING PMT AND DIGITAL IMAGING TUTORIALS

<http://www.olympusfluoview.com/theory/pmtintro.html>
<http://www.microscopyu.com/articles/digitalimaging/digitalintro.html>
<http://www.olympusmicro.com/primer/digitalimaging/>
<http://www.emccd.com/tutorial.htm>

estimate read noise (N_{read}), take a 0-s exposure and again calculate the SD across the image. Finally, the dark noise (N_{dark}) can be calculated from

$$N_{\text{camera}}^2 = N_{\text{read}}^2 + N_{\text{dark}}^2 \quad (4)$$

For comparative purposes, read noise is expressed in electrons/pixel and dark current in electrons/pixel/second. To convert A/D output intensity values to electrons, use the gain value supplied by the manufacturer. Alternatively, if the A/D range and the full well capacity (FWC) of the chip are properly matched, divide by the range of the A/D converter (e.g., 12-bit is $2^{12} = 4096$) and multiply by FWC (e.g., 18,500 electrons /pixel for the Orca II ER). Now calculate dark current (D) from

$$D = N_{\text{dark}}^2 / t \quad (5)$$

where t is the exposure duration used to measure N_{dark} . The most critical parameter for comparative purposes is dark current, as single-cell luminescence usually requires long exposure times (i.e., 15–60 min).

Perhaps the best currently available detector for single-cell luminescence is the cooled, back-thinned CCD camera. This device was originally developed for astronomy applications, such as detecting dim stars on a dark background, where very long exposures are practical because the target does not change quickly. In the back-thinned design, the chip is thinned to transparency so that it can be illuminated from behind, and photons do not have to pass through the electron channeling structures on the front of the chip. An antireflection coating is applied to the exposed surface of the chip. This design increases the QE to $\sim 95\%$ at 560 nm. At the slowest readout speed (which minimizes read noise by reducing electronic bandwidth), such chips should have read noise of only ~ 3 electrons.

Cooling the CCD to temperatures of -80 to -100° greatly reduces thermal dark current ($< 10^{-3}$ electrons/pixel/s). Traditionally, such low temperatures were achieved using liquid nitrogen, but long-term imaging requires daily refilling, and thermoelectric (Peltier) cooling is more practical. Convection, fans, or circulating liquid is used to draw heat from the Peltier elements. It is important that CCD cooling be independent of ambient temperature variations. With one camera, we found a small diurnal variation in dark current that correlated with ambient temperature fluctuations in the building. Warming and recooling the CCD may be advisable after bright-field imaging; this may reduce dark current by clearing residual charge. We have tested cooled, back-thinned CCD cameras made by Andor Technology, Roper Scientific, and Spectral Instruments, and all perform well for single-cell luminescence imaging, with higher QE and lower dark current than the Orca II ER (Hamamatsu) we used initially.

Another option is the photon-counting intensified CCD (iCCD) camera, such as the VIM system we use for plant imaging (see earlier discussion). These cameras were originally developed for military applications requiring rapid imaging of dimly lit moving objects. In the latest designs, a miniature array of photomultipliers, known as a microchannel plate (MCP), or intensifier, preamplifies the input signal before it reaches the CCD, which is now used mainly as a readout device. The QE of the best iCCD intensifiers ($\sim 40\text{--}50\%$) is much lower than that of back-thinned CCDs. However, because the CCD read noise is negligible due to preamplification, there is no penalty for taking more frequent, shorter exposures, and both the photocathode of the intensifier and the CCD itself can be cooled, resulting in very low dark current comparable to conventional cooled CCDs. An additional source of noise in these detectors arises from random fluctuations in intensifier gain, but this can be reduced using two MCPs in series so that their fluctuations tend to cancel. For dim luminescence, iCCD cameras are best operated in a "photon-counting" mode, such that (rare) individual photon events are saturating. In this mode, exposure times must be kept relatively short (e.g., 1 s) so that the chance of overlapping photon events is minimal. However, useful images may require summing many minutes of data, and this obviously presents some data-processing challenges for long-term experiments. Another disadvantage is that iCCDs, like PMTs, are vulnerable to damage if exposed to high light levels. We tested one new photon-counting iCCD camera, the XR/MEGA-10Z (Stanford Photonics), and it compares favorably with conventional cooled CCD cameras for single-cell luminescence imaging.

Several other CCD technologies are potentially suitable for low-light luminescence imaging. The electron bombardment CCD (EB-CCD) is similar to an iCCD, except that preamplification is achieved by placing the CCD inside a single large, high-voltage photomultiplier instead of downstream from an array of tiny ones (the MCP). The electron-multiplying CCD (EM-CCD) is a CCD in which electrons are multiplied on the chip itself before they are read out. This is done by passing electrons through a "gain register" portion of the chip using very high voltages so that, occasionally, a fast-moving electron causes impact ionization as it is transferred, resulting in additional mobile electrons. Thus, like the iCCD, both of these technologies preamplify the signal so that CCD read noise is negligible by comparison, and very fast frame rates are possible at low light levels. However, at the extremely low signal levels of single-cell luminescence imaging, where longer integration times are required, dark noise dominates over read noise. We are unaware of any EB-CCD or EM-CCD cameras with dark current as low as conventional cooled CCD cameras.

Temporal and Spatial Resolution

For a given sample and a given detector, one can still improve the S/N by measuring more photons, at the expense of either temporal or spatial resolution. One can increase exposure time, sample a greater area per pixel using a lower-power objective, or combine adjacent pixels (binning). When photons are gathered over a longer time or from a wider area, the signal increases proportionally, but most types of noise do not:

$$N_{\text{total}}^2 = N_{\text{shot}}^2 + N_{\text{dark}}^2 + N_{\text{read}}^2 \quad (6)$$

The random statistical fluctuation of the signal (“shot noise”) increases only as the square root of the number of photons. Dark current increases in proportion to the signal for longer exposure times or binning, but not for lower magnification. Therefore, dark noise (which is really just shot noise for the dark current) increases only as the square root of the signal for longer exposures or binning, and does not increase at all with lower magnification. Read noise does not increase at all with integration time, decreased magnification, or “on-chip” binning (in which electrons from an array of pixels are read out collectively, as if they were from a single pixel). Fortunately, the inherent temporal dynamics of circadian rhythms are quite slow, such that 15–30 min of resolution is more than adequate, and only very coarse spatial resolution is required to discriminate one cell from another. Thus, even extremely dim circadian reporters may be useful at low temporal and spatial resolution.

Data Analysis

Image Correction

Postprocessing of images can correct for certain imperfections in the CCD detector. First, for each readout mode of a CCD camera (i.e., binning, readout rate), there is an associated pattern of current at zero exposure duration, which is known as a bias image. Second, for a given readout mode and nonzero exposure duration in the dark, there is a pattern of dark current (in excess of the bias current), which is known as a dark image. Third, for a given exposure duration and a uniformly illuminated field, there is a nonuniform pattern of current (arising from nonuniform QE), known as a flat field image. For the flat field image, illumination should be perfectly uniform, near half-saturating in intensity, and similar to luciferase luminescence in spectral composition. We use green luminescent liquid from commercial “light sticks” (Extreme Glow) in a 35-mm culture dish. Low-noise bias, dark, and flat field images should be created by averaging multiple exposures of the

appropriate type. Then, for each data image: (1) subtract the bias image, (2) subtract a dark image (scaled by exposure time if necessary), and (3) multiply all pixels by the average intensity of the flat field image and then divide (pixelwise) by the flat field image. Any experimental image can be improved by correcting for these three types of CCD imperfections.

Bright Spots

Bright spot artifacts are common in CCD images. Some of these are consistent from one exposure to the next and may result from light-scattering dust or scratches on glass surfaces in the optical path or from imperfections in the CCD itself (“hot pixels”). Such consistent artifacts can be removed from data images by subtracting a background image or by two-dimensional (2D) interpolation. Larger, extremely bright spots appearing sporadically in long exposures ($\sim 100/h$, in random image locations) are “cosmic ray artifacts,” or “spurious events.” Radioactive laboratory reagents, concrete, or radon gas are possible sources of ionizing radiation producing such artifacts and should be kept away from the CCD camera. Another significant source is K-40, a naturally occurring isotope of potassium. CCD chip anomalies can also cause spurious events. But many of the spots really do result from “cosmic rays”: a stream of particles of extraterrestrial origin (e.g., muons, protons), which liberate electrons when they strike the CCD chip. The imaging setup could be protected from some cosmic rays by lead shielding, but this is usually impractical. Instead, cosmic ray artifacts are generally removed by image processing: median filtering or 2D interpolation within a single image or averaging adjacent images from a time series. One sensible approach is to collect images more frequently than the desired final temporal resolution and then average each set of two to three adjacent images while excluding pixels brighter than a threshold value. An even simpler algorithm is to use the minimum value for each pixel among the two to three adjacent images (although this throws away the improved S/N gained by averaging).

MetaMorph

Images are then analyzed using MetaMorph software (Universal Imaging Corp.). For each image, average luminescence intensity is measured within a region of interest defined manually for each plant or cell. The position of the region is adjusted if necessary to accommodate movements of cells during the experiment, but its size is kept constant across the time series. Our “Import and Analysis” (I and A) macro tool (<http://www.scripps.edu/cb/kay/ianda>) facilitates import of long time series into a Microsoft Excel file for further analysis.

χ^2 Periodogram

There are several reasonable approaches to analyzing circadian rhythm data (Refinetti, 1993). Perhaps the simplest approach is the χ^2 periodogram (Sokolove and Bushell, 1978). In this method, raw data are simply folded at various candidate periods in the circadian range (i.e., averaging together points 20.0 h apart, 20.1 h apart, etc.), and the period producing the average waveform with the greatest amplitude is selected. Amplitude is defined as the variance or SD of the values in the folded waveform. For circadian phase determinations, data can be smoothed using a 2-h moving average. Circadian phase is then defined by the time of the smoothed peak or trough of the rhythm. The χ^2 periodogram has the advantage of making no assumptions about circadian rhythm waveform and is therefore valid for any type of circadian rhythm data. Fortunately, however, luminescence rhythms are usually nicely approximated by damped sine or cosine curves; methods based on fitting data to such curves can provide more statistically tractable estimates of rhythm parameters.

FFT-NLLS

For plant data, we use a method developed by Marty Straume at University of Virginia, known as fast Fourier transform-nonlinear least-squares analysis (FFT-NLLS) (Plautz *et al.*, 1997; Straume *et al.*, 1991). In this method, data are fitted to a series of linearly damped cosine curves with linear baseline drift:

$$L(t) = (c_0 + c_1t) + (A_0 + A_1t) \cdot \cos(2\pi t/\tau - \phi) + \dots \quad (7)$$

where L is luminescence intensity, t is time, c_0 is luminescence at $t = 0$, c_1 is linear rate of change of luminescence with time, A_0 is amplitude at $t = 0$, A_1 is linear rate of change of amplitude with time, τ is circadian period, and ϕ is circadian phase. Additional terms from the Fourier analysis are added until there is no significant residual amplitude. In this analysis, the amplitude of the residuals relative to the primary fitted amplitude (relative amplitude, or “Rel Amp”) is a useful metric of rhythm significance, varying from 0 (perfect cosine fit) to 1 (residual amplitude equals fitted amplitude). With this method, joint confidence limits can be estimated for all parameters at a criterion of 95% probability.

LumiCycle Analysis

For mammalian data, we use the data analysis package accompanying the LumiCycle luminometer developed by David Ferster (Actimetrics). In this method, baseline fluctuations fit to a polynomial curve are first

subtracted from raw data, and subtracted data are then fit to a single sine wave with exponentially decaying amplitude:

$$L(t) = A_0 \cdot e^{-t/k} \cdot \sin(2\pi t/\tau - \phi) \quad (8)$$

where L is luminescence intensity, t is time, A_0 is amplitude at $t = 0$, k is time constant for exponential decay of amplitude, τ is circadian period, and ϕ is circadian phase. This method produces better results for mammalian data, which sometimes show complex baseline fluctuations and rapid damping that is modeled more accurately by exponential decay than by the linear damping assumed in FFT-NLLS.

Acknowledgments

We thank Elisabeth Gardiner and Kathy Spencer for expert microscopy support. We thank Andrew Liu, Tom Schultz, and Gary Sims for thoughtful comments on the manuscript. Supported in part by K08 MH067657 (DKW) and MH51573 (SAK).

References

- Asai, M., Yamaguchi, S., Isejima, H., Jonouchi, M., Moriya, T., Shibata, S., Kobayashi, M., and Okamura, H. (2001). Visualization of *mPer1* transcription *in vitro*. *Curr. Biol.* **11**, 1524–1527.
- Bae, K., Jin, X., Maywood, E. S., Hastings, M. H., Reppert, S. M., and Weaver, D. R. (2001). Differential functions of *mPer1*, *mPer2*, and *mPer3* in the SCN circadian clock. *Neuron* **30**, 525–536.
- Billinton, N., and Knight, A. W. (2001). Seeing the wood through the trees: A review of techniques for distinguishing green fluorescent protein from endogenous autofluorescence. *Anal. Biochem.* **291**, 175–197.
- Brandes, C., Plautz, J. D., Stanewsky, R., Jamison, C. F., Straume, M., Wood, K. V., Kay, S. A., and Hall, J. C. (1996). Novel features of *Drosophila period* transcription revealed by real-time luciferase reporting. *Neuron* **16**, 687–692.
- Christenson, M. A. (2002). Detection systems optimized for low-light chemiluminescence imaging. In “Luminescence Biotechnology: Instruments and Applications” (K. Van Dyke, C. Van Dyke, and K. Woodfork, eds.), pp. 469–480. CRC Press, Boca Raton, FL.
- Clough, S. J., and Bent, A. F. (1998). Floral dip: A simplified method for *Agrobacterium*-mediated transformation of *Arabidopsis thaliana*. *Plant J.* **16**, 735–743.
- Greer, L. F., 3rd, and Szalay, A. A. (2002). Imaging of light emission from the expression of luciferases in living cells and organisms: A review. *Luminescence* **17**, 43–74.
- Hamada, T., LeSauter, J., Venuti, J. M., and Silver, R. (2001). Expression of *Period* genes: Rhythmic and nonrhythmic compartments of the suprachiasmatic nucleus pacemaker. *J. Neurosci.* **21**, 7742–7750.
- Hastings, J. W. (1989). Chemistry, clones, and circadian control of the dinoflagellate bioluminescent system. The Marlene DeLuca memorial lecture. *J. Biolumin. Chemilumin.* **4**, 12–19.
- Ikeda, M., Sugiyama, T., Wallace, C. S., Gompf, H. S., Yoshioka, T., Miyawaki, A., and Allen, C. N. (2003). Circadian dynamics of cytosolic and nuclear Ca^{2+} in single suprachiasmatic nucleus neurons. *Neuron* **38**, 253–263.

- Kondo, T., Strayer, C. A., Kulkarni, R. D., Taylor, W., Ishiura, M., Golden, S. S., and Johnson, C. H. (1993). Circadian rhythms in prokaryotes: Luciferase as a reporter of circadian gene expression in cyanobacteria. *Proc. Natl. Acad. Sci. USA* **90**, 5672–5676.
- Kuhlman, S. J., Quintero, J. E., and McMahon, D. G. (2000). GFP fluorescence reports *Period 1* circadian gene regulation in the mammalian biological clock. *Neuroreport* **11**, 1479–1482.
- Lai, C. M., Lai, Y. K., and Rakoczy, P. E. (2002). Adenovirus and adeno-associated virus vectors. *DNA Cell Biol.* **21**, 895–913.
- Leclerc, G. M., Boockfor, F. R., Faught, W. J., and Frawley, L. S. (2000). Development of a destabilized firefly luciferase enzyme for measurement of gene expression. *Biotechniques* **29**, 590–598.
- Le Gal La Salle, G., Robert, J. J., Berrard, S., Ridoux, V., Stratford-Perricaudet, L. D., Perricaudet, M., and Mallet, J. (1993). An adenovirus vector for gene transfer into neurons and glia in the brain. *Science* **259**, 988–990.
- Millar, A. J., Short, S. R., Chua, N. H., and Kay, S. A. (1992). A novel circadian phenotype based on firefly luciferase expression in transgenic plants. *Plant Cell* **4**, 1075–1087.
- Plautz, J. D., Straume, M., Stanewsky, R., Jamison, C. F., Brandes, C., Dowse, H. B., Hall, J. C., and Kay, S. A. (1997). Quantitative analysis of *Drosophila period* gene transcription in living animals. *J. Biol. Rhythms* **12**, 204–217.
- Refinetti, R. (1993). Laboratory instrumentation and computing: Comparison of six methods for the determination of the period of circadian rhythms. *Physiol. Behav.* **54**, 869–875.
- Sokolove, P. G., and Bushell, W. N. (1978). The chi square periodogram: Its utility for analysis of circadian rhythms. *J. Theor Biol.* **72**, 131–160.
- Straume, M., Frasier-Cadoret, S. G., and Johnson, M. L. (1991). Least-squares analysis of fluorescence data. “Topics in Fluorescence Spectroscopy” (J. R. Lakowicz, ed.), Vol. 2, pp. 117–240. Plenum, New York.
- Strayer, C., Oyama, T., Schultz, T. F., Raman, R., Somers, D. E., Mas, P., Panda, S., Kreps, J. A., and Kay, S. A. (2000). Cloning of the *Arabidopsis* clock gene TOC1, an autoregulatory response regulator homolog. *Science* **289**, 768–771.
- Welsh, D. K., Yoo, S.-H., Liu, A. C., Takahashi, J. S., and Kay, S. A. (2004). Bioluminescence imaging of individual fibroblasts reveals persistent, independently phased circadian rhythms of clock gene expression. *Curr. Biol.* **14**, 2289–2295.
- Wilsbacher, L. D., Yamazaki, S., Herzog, E. D., Song, E. J., Radcliffe, L. A., Abe, M., Block, G., Spitznagel, E., Menaker, M., and Takahashi, J. S. (2002). Photic and circadian expression of luciferase in *mPeriod1-luc* transgenic mice *in vivo*. *Proc. Natl. Acad. Sci. USA* **99**, 489–494.
- Yamaguchi, S., Isejima, H., Matsuo, T., Okura, R., Yagita, K., Kobayashi, M., and Okamura, H. (2003). Synchronization of cellular clocks in the suprachiasmatic nucleus. *Science* **302**, 1408–1412.
- Yamaguchi, S., Kobayashi, M., Mitsui, S., Ishida, Y., van der Horst, G. T., Suzuki, M., Shibata, S., and Okamura, H. (2001). View of a mouse clock gene ticking. *Nature* **409**, 684.
- Yamazaki, S., Numano, R., Abe, M., Hida, A., Takahashi, R., Ueda, M., Block, G. D., Sakaki, Y., Menaker, M., and Tei, H. (2000). Resetting central and peripheral circadian oscillators in transgenic rats. *Science* **288**, 682–685.
- Yoo, S. H., Yamazaki, S., Lowrey, P. L., Shimomura, K., Ko, C. H., Buhre, E. D., Slepka, S. M., Hong, H. K., Oh, W. J., Yoo, O. J., Menaker, M., and Takahashi, J. S. (2004). PERIOD2::LUCIFERASE real-time reporting of circadian dynamics reveals persistent circadian oscillations in mouse peripheral tissues. *Proc. Natl. Acad. Sci. USA* **101**, 5339–5346.
- Zhang, J., Campbell, R. E., Ting, A. Y., and Tsien, R. Y. (2002). Creating new fluorescent probes for cell biology. *Nat. Rev. Mol. Cell Biol.* **3**, 906–918.

- Zheng, B., Albrecht, U., Kaasik, K., Sage, M., Lu, W., Vaishnav, S., Li, Q., Sun, Z. S., Eichele, G., Bradley, A., and Lee, C. C. (2001). Nonredundant roles of the mPer1 and mPer2 genes in the mammalian circadian clock. *Cell* **105**, 683–694.
- Zylka, M. J., and Schnapp, B. J. (1996). Optimized filter set and viewing conditions for the S65T mutant of GFP in living cells. *BioTechniques* **21**, 220–226.

[12] Real-Time Luminescence Reporting of Circadian Gene Expression in Mammals

By SHIN YAMAZAKI and JOSEPH S. TAKAHASHI

Abstract

Luminescence reporters have been used successfully in studies of circadian rhythms. Real-time measurements of circadian variations in gene expression were made in living cells, cultured tissues, and whole organisms. Because this technique is relatively easy and continuous noninvasive measurement from tissue cultures allows for a drastic reduction in the number of experimental animals, we believe this method will become a common technique for studying circadian rhythms. Using a multichannel recording apparatus, it may also become a powerful tool for the discovery of new drugs. In the past, measurements were done using hand-made apparatuses or by modifying commercially available equipment. We, along with other investigators, have developed user-friendly equipment for performing circadian rhythms experiments, and these systems are now available commercially. This article describes the use of luminescence reporters in circadian research and provides detailed methods used in these experiments. One of our goals in this article is to reduce experimental variability in different laboratories by proposing standard protocols.

Introduction

Ever since luciferase was introduced in real-time luminescence monitoring of gene expression rhythms in plants and cyanobacteria (Kondo *et al.*, 1993; Millar *et al.*, 1992), luminescence reporter techniques have become a powerful tool used in noninvasive assays of circadian oscillations. This method has faithfully monitored the rhythms of circadian genes in the fly (Brandes *et al.*, 1996), mouse (Asai *et al.*, 2001; Geusz *et al.*, 1997; Wilsbacher *et al.*, 2002; Yoo *et al.*, 2004), rat (Yamazaki *et al.*, 2000), and fungi (Morgan *et al.*, 2003), as well as immortalized cell lines driven from the rat (Izumo *et al.*, 2003; Ueda *et al.*, 2002), zebrafish (Vallone *et al.*,